

# COMPENSATION OF INSERTION DEVICE INDUCED EMITTANCE VARIATIONS IN ULTRALOW EMITTANCE STORAGE RINGS BY A DISPERSION BUMP IN A WIGGLER\*

F. Sannibale<sup>†</sup>, M. Ehrlichman, T. Hellert, S. C. Leemann, D. S. Robin,  
 C. A. Steier, C. Sun, M. Venturini,  
 Lawrence Berkeley National Laboratory, Berkeley, 94720 CA, USA.

## Abstract

Multi-bend achromat lattices allow for the design of extremely low emittance electron storage rings and hence for the realization of extremely high-brightness X-ray photon sources. In these new rings, the beam energy lost to radiation in the insertion devices (IDs) is often comparable to that lost in the ring dipole magnets. This implies that with respect to the typical 3rd generation light source, these new machines are more sensitive to the energy loss variations randomly occurring as the many users independently operate the gap of their IDs. The consequent induced variations in radiation damping time, equilibrium emittance, and transverse beam sizes at the radiation point sources can be significant and degrade the experimental performance in some of the beamlines. In this paper we describe and discuss a possible method to compensate for such emittance variations by using a variable dispersion bump localized inside a fixed gap wiggler.

## INTRODUCTION

In the last decade, technological progress and improved beam dynamics calculation techniques made the construction of storage rings using Multi Bend Achromat (MBA) lattices possible. The extremely low emittances achievable with such schemes (more than an order of magnitude with respect to the present 3rd generation light sources) allows for ring-based light sources with often several orders of magnitude increase in terms of brightness. A number of upgraded and new light sources based on MBA schemes were proposed, some funded and the successful commissioning and first operation of MAX IV in Sweden [1] confirmed the capability of the scheme of delivering the promised results.

The low emittance performance of MBA lattices is obtained by strong transverse focusing and large bending radii in dipole magnets to control and reduce dispersion in the arcs. Unlike in present 3rd generation light sources, the large bending radius of MBA-based rings significantly decreases the amount of energy radiated in the bends, making it comparable to that radiated in the insertion devices (IDs). Consequently, insertion devices can significantly impact the equilibrium emittance of an MBA-based ring. When ID gaps are independently adjusted by users during normal

operation, the resulting modulation of the total radiated energy results in variations of the beam damping time, of the electron beam emittance, and ultimately changes the photon distribution in the beamlines [2]. This is especially true for short wavelengths, where far from diffraction limit, the photons reproduce the electron distribution with fidelity. Some of the beamline experiments, for example those based on scanning transmission X-ray microscopy (STXM), are very sensitive to variations of the transverse photon distribution and the quality of their experiments can be significantly affected if those variations are not compensated. Estimates for the particular case of the ALS-U, the MBA upgrade of the Advanced Light Source (ALS) at Lawrence Berkeley National Laboratory [3], indicate that up to ~7% (4 sigma) ID-induced emittance variations can be expected [4]. This value is large enough to require an active compensation scheme to preserve the quality of the experiments in those sensitive beamlines.

A number of different methods that could be used for compensating for these emittance variations, with their pros and cons, were discussed elsewhere [4]. In this paper we concentrate on the analysis of the scheme that uses a variable horizontal dispersion bump inside a fixed gap wiggler to compensate for the emittance variations. According to the analysis in [4] this appears to be the most efficient and workable approach as it is compatible with user operation of the wiggler (wiggler typically works at fixed gap for users), is relatively simple to implement and does not affect the performance of the ring in any of its other deliverables. In this paper, the v20r baseline ALS-U lattice is used to demonstrate the technique.

## THEORY

Assume that a wiggler is located at the center of the straight section of a storage ring. The horizontal optical functions in the straight section are then given by:

$$\beta_x = \beta_{wx} \left( 1 + \frac{s^2}{\beta_{wx}^2} \right), \quad \alpha_x = -\frac{s}{\beta_{wx}}, \quad \gamma_x = \frac{1}{\beta_{wx}} \quad (1)$$

where  $\alpha_x$ ,  $\beta_x$  and  $\gamma_x$  are the horizontal plane Twiss parameters,  $s$  is the longitudinal coordinate with  $s = 0$  at the center of the straight section, and  $\beta_{wx}$  is the value of the beta function at the waist located at  $s = 0$ .

The natural emittance  $\epsilon_0$  of a ring is given by [5]:

$$\epsilon_0 = C_q \frac{\gamma^2 I_5}{J_x I_2} \quad \text{with} \quad J_x = 1 - \frac{I_4}{I_2} \quad (2)$$

\* Work supported by the Director of the Office of Science of the US Department of Energy under Contract no. DEAC02-05CH11231.

<sup>†</sup> FSannibale@lbl.gov

where  $\gamma$  is the beam energy in rest mass units,  $J_x$  is the horizontal partition number and  $C_q$  is a constant with value  $3.832 \times 10^{-13}$  m.  $I_2$ ,  $I_4$  and  $I_5$  are the synchrotron integrals:

$$I_5 = \oint \frac{\mathcal{H}}{|\rho|^3} ds, \quad \mathcal{H} = \gamma_x \eta_x^2 + 2\alpha_x \eta_x \eta'_x + \beta_x \eta'^2_x \quad (3)$$

$$I_2 = \oint \frac{ds}{\rho^2}, \quad I_4 = \oint \frac{\eta_x}{\rho} \left( \frac{1}{\rho^2} + 2k_1 \right) ds, \quad (4)$$

where  $\eta_x$  and  $\eta'_x$  are the dispersion and its derivative with respect to  $s$ ,  $\rho$  is the radius of curvature and  $k_1$  is the derivative of the magnetic field with respect to the horizontal direction  $x$ .

The emittance contribution from a dispersion bump in a wiggler is found by integrating  $I_5$ ,  $I_2$ , and  $I_4$  through the wiggler. There are two contributions to the dispersion inside a wiggler, one from the storage ring, and one induced by the wiggler itself,

$$\eta_x = \eta_{0x} - \left( \frac{\lambda_W}{2\pi} \right)^2 \frac{\hat{B}_W^2}{(B\rho)^2} \sin \frac{2\pi}{\lambda_W} s, \quad (5)$$

where  $\eta_{0x}$  is the storage ring contribution,  $\lambda_W$  is the wiggler period,  $\hat{B}_W$  is the wiggler field peak value ( $B_W = \hat{B}_W \sin 2\pi s/\lambda_W$ ), and  $(B\rho) = (\gamma^2 - 1)^{1/2} mc$  is the rigidity of the beam, with  $m$  the electron rest mass and  $c$  the speed of light. In our horizontal dispersion bump case, we assume  $\eta_{0x}$  constant inside the wiggler which implies  $\eta'_{0x} = 0$ .

From equations (1), (3) (5) and assuming  $k_1 = 0$  inside the wiggler, one can derive the contribution of the dispersion bump to the three synchrotron integrals:

$$\Delta I_{2W}^{\eta_{x0}}, \Delta I_{4W}^{\eta_{x0}} = 0 \rightarrow \Delta J_{xW}^{\eta_{x0}} = 0, \quad (6)$$

$$\Delta I_{5W}^{\eta_{x0}} = \frac{4}{3\pi} \frac{\hat{B}_W^3}{(B\rho)^3} \frac{L_W}{\beta_{wx}} \eta_{x0}^2, \quad (7)$$

where  $L_W$  is the wiggler length.

Using equations (2), (6) and (7) one can conclude that the relative emittance variation associated with the dispersion bump is given by:

$$\frac{\Delta \varepsilon}{\varepsilon_0} = \frac{\Delta J_{5W}^{\eta_{x0}}}{I_5} \quad (8)$$

where  $I_5$  is calculated over the whole ring.

## SIMULATION USING THE ALS-U CASE

In order to apply the compensation technique to a realistic case, the ALS-U baseline lattice v20r is used [3]. Figure 1 shows the optical functions of this 9BA lattice and Table 1 its main parameters. While the ALS-U will probably contain superbends (high field dipole magnets in the arcs), for sake of simplicity they are not included in this particular lattice model.

First, we will verify the validity of (7) using the ELEGANT code [6] to simulate the case of the wiggler presently operating at the ALS (also to be used in ALS-U). For the beta function at the waist we used the value of 2.048 m

of the ALS-U v20r lattice. Figure 2 shows how the simulation results nicely agrees with the analytical prediction of equation (7).

The next step is to assume a simple four-dipole chicane layout for generating the dispersion bump in the wiggler as shown in the cartoon at the bottom of Fig. 3. In this (non optimized) configuration, the four identical bend magnets are 0.15 m long and need to generate a field of  $\sim 0.9$  T for a 1 cm dispersion bump. Such magnets are realistic although a further optimization of the chicane parameter could provide a weakest field configuration.

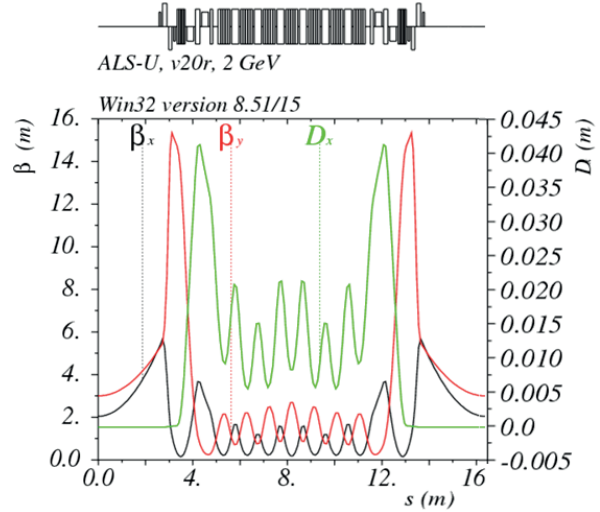


Figure 1: ALS-U v20r lattice optical functions.

Table 1: Main Parameters for the ALS-U Lattice v20r

Parameter	Value	Unit
Energy	2	GeV
Number of bends per period/ number of periods	9/12	
Ring length	196.5	m
Nominal RF frequency	500	MHz
Harmonic number	328	
Charge per bunch	1.154	nC
Total average current	500	mA
Reverse bends?	Yes in 7 out of 9 bends	
Super bends?	No	
Natural emittance	91.76	pm
Hor./Vert. emitt. with IBS at full coupling	70/70	pm
Hor./Vert. emitt. with IBS at full coupling and IDs	63/63	pm
Betatron tunes (H/V)	41.35/20.35	
Beta functions at the straight section center (H/V)	2.048/2.998	m
R.m.s. bunch length with IBS and harmonic cavities	112	ps
Energy spread (w / w/o IBS)	0.094/0.102	%
Energy lost/turn (no IDs)	217.24	keV
Hor. partition number (no IDs)	2.0838	
Momentum compaction	$2.116 \cdot 10^{-4}$	

Figure 3 also shows the optical functions and the dispersion bump in the wiggler straight that is generated using the chicane.

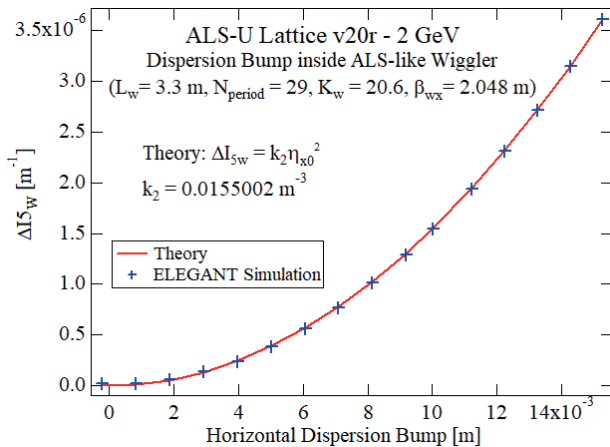


Figure 2: Contribution of the dispersion bump in the ALS-like wiggler to  $I_5$  integral. Analytical prediction from equation (8) are compared with simulation results.

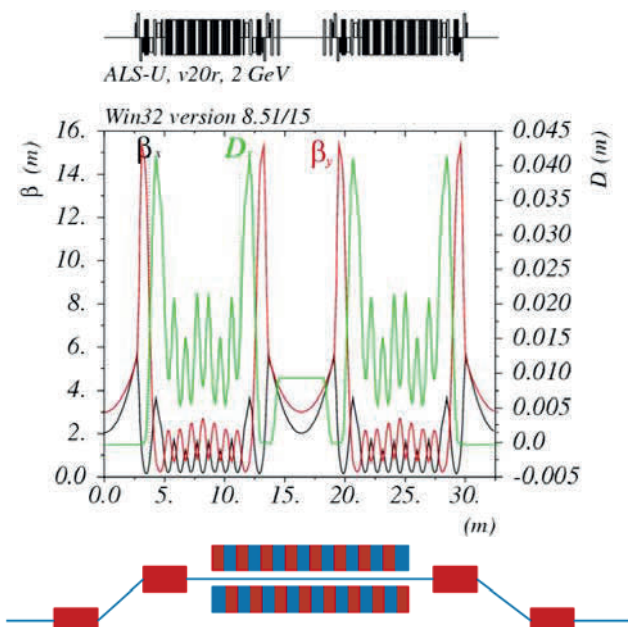


Figure 3: Simulation showing the dispersion bump in the wiggler straight section created by the four dipole chicane sketched at the bottom of the figure. Chicane and wiggler are fully contained within the straight section length.

Figure 4 shows the result of the simulation where the emittance variations for the ALS-U v20r lattice are calculated when the magnitude of the dispersion bump in the wiggler is varied. One can see that in order to compensate for the estimated ID-induced emittance variations of  $\sim 7\%$  for the ALS-U case, one has to consider dispersion bumps as large as  $\sim 1$  cm. The 4th power dependence of the emittance on the dispersion bump amplitude shown in Fig.4 is stronger than the quadratic dependence predicted by equation (7).

This is due to the fact that the chicane itself generates a significant emittance contribution as it is clearly shown in Fig. 5.

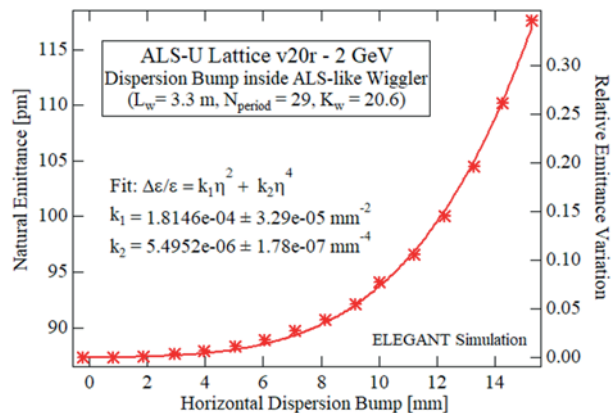


Figure 4: Simulation showing the dependence of the emittance on the dispersion bump amplitude inside the ALS-like wiggler for the ALS-U v20r case. The dispersion bump is created by the four-dipole chicane shown in Fig.3.

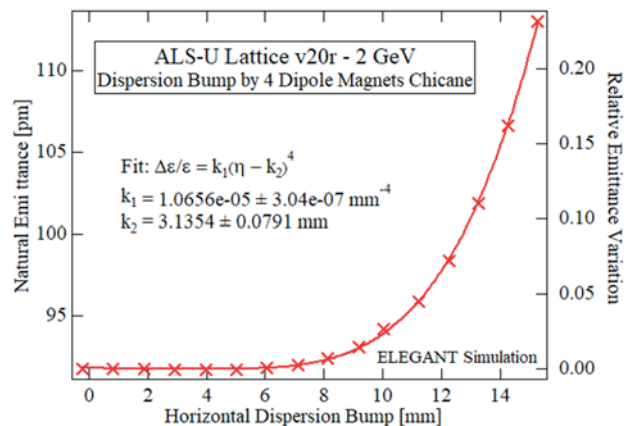


Figure 5: Simulation showing the emittance contribution due to the four-dipole chicane itself.

## CONCLUSIONS

The compensation for insertion device driven emittance variations by a variable horizontal dispersion bump inside a fixed gap wiggler was studied. This first analysis indicates that the method is feasible and could be potentially used in the case of the ALS-U, the underway MBA upgrade of the Advanced Light Source at Berkeley.

The simple implementation of the method using a four-dipole chicane to create the dispersion bump requires strong but realistic bend magnets. Further optimization of the chicane can potentially decrease the required magnetic field. Alternatively, the bump could be created by detuning the optical functions in the two sectors adjacent to the wiggler.

A machine learning application, similar to the one being successfully implemented at the ALS for the stabilization of the transverse beam size [7], could be used in this scheme as well for controlling the compensation process.

## REFERENCES

- [1] S. C. Leemann, M. Sjöström, and Å. Andersson, "First optics and beam dynamics studies on the MAX IV 3 GeV storage ring", *Nucl. Instrum. Meth. A* **883** 33–47, 2018.
- [2] See for example: S. C. Leemann, "Interplay of Touschek scattering, intrabeam scattering, and rf cavities in ultralow-emittance storage rings", *Phys. Rev. ST Accel. Beams* **17**, 050705, 2014.
- [3] C. Steier *et al.*, "Design Progress of ALS-U, the Soft X-Ray Diffraction Limited Upgrade of the Advanced Light Source", presented at the 10th Int. Particle Accelerator Conf. (IPAC'19), Melbourne, Australia, May 2019, paper TUPGW097, this conference.
- [4] F. Sannibale *et al.*, "Compensation of Insertion Device Induced Emittance Variations in Ultralow Emittance Storage Rings", in *Proc. 9th Int. Particle Accelerator Conf. (IPAC'18)*, Vancouver, Canada, Apr.-May 2018, pp. 1751-1754. doi:10.18429/JACoW-IPAC2018-WEXGBE2
- [5] See for example: A. Wolski, "Low emittance storage rings", CERN-2014-009, pp. 245-294, or arXiv:1507.02213 [physics.acc-ph].
- [6] M. Borland, "ELEGANT: A Flexible SDDS-Compliant Code for Accelerator Simulation," Advanced Photon Source LS-287, September 2000.
- [7] S. C. Leemann *et al.*, "First Attempts at Applying Machine Learning to ALS Storage Ring Stabilization", presented at the 10th Int. Particle Accelerator Conf. (IPAC'19), Melbourne, Australia, May 2019, paper TUPGW094, this conference.